Kelvin-wave cascade and dissipation in low-temperature superfluid vortices

Giorgio Krstulovic

Laboratoire Lagrange, UMR7293, Université de Nice Sophia-Antipolis, CNRS, Observatoire de la Côte d'Azur,
B.P. 4229, 06304 Nice Cedex 4, France

We study the statistical properties of the Kelvin waves propagating along quantized superfluid vortices driven by the Gross-Pitaevskii equation. No artificial forcing or dissipation is added. Vortex positions are accurately tracked. This procedure directly allows us to obtain the Kevin-wave occupation-number spectrum. Numerical data obtained from long time integration and ensemble average over initial conditions support the spectrum proposed in L'vov and Nazarenko [JETP Lett. **91**, 428 (2010)]. Kelvin-wave modes in the inertial range are found to be Gaussian as expected by weak-turbulence predictions. Finally the dissipative range of the Kelvin-wave spectrum is studied. Strong non-Gaussian fluctuations are observed in this range.

Superfluid turbulence has been the subject of many experimental and theoretical works for the last decades. It is now possible to realize turbulent Bose-Einstein condensates (BECs) [1], turbulent flows with ^{3}He [2,3], and visualize vortices in ^{4}He [4]. As in classical turbulence [5], a Kolmogorov energy cascade has been observed experimentally and numerically. In superfluids, this takes place at scales larger than the mean intervortex distance ℓ [6–8]. At low temperature, when damping due to mutual friction is negligible, it is believed that dissipation at small scales is carried by phonon radiation which dissipates energy into heat [9]. At scales smaller than ℓ the energy is transferred down by a series of reconnection processes of quantized vortices that excite waves on the filaments. These perturbations, called Kelvin waves (KWs), are known for more than one century [10] in fluid dynamics. These waves obey a set of nonlinear equations where the energy is transferred towards small scales by a wave-turbulence cascade. The energy distribution along different scales is crucial for the understanding of the dissipative processes in superfluids. The energy spectrum of such a cascade is not yet fully determined, except in the limit of small-amplitude KWs, where the theory of weak turbulence is applicable [11]. However, a heated debate on the locality of KW energy transfer has taken place in the last years [12–17]. Two different groups, Kozik and Svistunov [18] and L'vov and Nazarenko [19], starting from the very same equations and by using the same theory, have derived two different spectra (hereafter KS and LN spectra, respectively). The origin of this controversy is mainly due to a symmetry argument by KS (tilt of a vortex line) that eventually leads to a vanishing vertex in the perturbative expansion. This leads to locality in the energy transfer and makes the six-wave interaction theory realizable. The energy spectrum found by KS is

$$E_{\text{KS}}(k) \sim \epsilon^{1/5} \kappa^{7/5} k^{-7/5}, \tag{1}$$

where ϵ is the energy flux, κ is the circulation quantum, and k is the wave vector. This symmetry argument was questioned by LN and they claimed that the energy transfer is nonlocal. They derived an effective four-wave interaction theory that leads to the energy spectrum

$$E_{\text{LN}}(k) \sim \kappa \epsilon^{1/3} \Psi^{-2/3} k^{-5/3}, \tag{2}$$

where $\Psi \sim (1/\kappa) \int E_{\text{LN}}(k)dk$ is the mean-square angular deviation of the vortex. For more technical details on the controversy see [13–17]. The exponent $7/5 = 1.4$ and $5/3 \approx 1.67$ of (1) and (2) are supposed to be universal, but their relatively close values makes it difficult to numerically elucidate which theory is correct. A number of numerical works supporting both theories have been published but none presenting strong arguments to settle this controversy [17,20,21]. These works are all done in the framework of the vortex filament with an *ad hoc* dissipative mechanism. In the case of strong wave turbulence, when the local slope of KW is order 1, weak turbulence breaks down and Vinen *et al.* [22] propose a spectrum scaling as k^{-1}. Finally, It was suggested by Sonin [16] that no universality can be expected.

In this Rapid Communication, we address the small-amplitude KW cascade problem by performing direct numerical simulations of the Gross-Pitaevskii equation (GPE). The GPE describes a weakly interacting BEC at low temperature. It is also expected to at least qualitatively reproduce the dynamics of superfluid helium. As the Gross-Pitaevskii (GP) vortices can naturally radiate and excite phonons no artificial dissipation is needed. The (1D) KW occupation-number spectrum is precisely obtained and data are found to support the wave-turbulence prediction (LN) [19]. The KW spectrum is analyzed within the dissipative range and an exponential decay is found. Finally, the probability distribution function (PDF) of KW amplitudes is observed to be Gaussian in the inertial range in contrast with the power-law tails observed for modes in the dissipative range.

The GPE describing a homogeneous BEC of volume V with wave function ψ is given by

$$i\hbar \frac{\partial \psi}{\partial t} = -\frac{\hbar^2}{2m}\nabla^2\psi + g|\psi|^2\psi, \tag{3}$$

where m is the mass of the condensed particles and $g = 4\pi a \hbar^2/m$, with a the s-wave scattering length. Equation (3) conserves the energy $H = \int(\frac{\hbar^2}{2m}|\nabla\psi|^2 + \frac{g}{2}|\psi|^4)d\mathbf{x}$ and the number of particles $N = \int |\psi|^2 d\mathbf{x}$. Madelung's transformation $\psi(\mathbf{x},t) = \sqrt{\frac{\rho(\mathbf{x},t)}{m}} \exp[i\frac{m}{\hbar}\phi(\mathbf{x},t)]$ relates the wave function ψ to a superfluid of density $\rho(\mathbf{x},t)$ and velocity $\mathbf{v} = \nabla\phi$, where $\kappa = h/m$ is the Onsager-Feynman quantum of velocity circulation around the $\psi = 0$ vortex lines. When Eq. (3) is

TABLE I. List of runs. $N_\perp$ and N_z are the resolutions in the perpendicular and parallel directions with respect to the vortex. N_{rea} is the number of realizations. n is the number of initial KW modes and m is the exponent k^{-m} of the KW spectrum.

Run	$N_\perp$	N_z	N_{rea}	n	ξ	A	m
I	256	128	31	3	0.025	2ξ	3.85 ± 0.24
II	256	128	31	2	0.025	4ξ	3.682 ± 0.13
III	256	256	11	2	0.025	4ξ	3.753 ± 0.17
IV	512	256	1	2	0.0125	4ξ	4.116 ± 0.56
V	128	512	11	2	0.1	4ξ	

linearized around a constant $\psi = \hat{\psi}_0$, the sound velocity is given by $c = (g|\hat{\psi}_0|^2/m)^{1/2}$ with dispersive effects taking

place at length scales smaller than the coherence length $\xi = (\hbar^2/2m|\hat{\psi}_0|^2 g)^{1/2}$ that also corresponds to the vortex core size. In this Rapid Communication the density $\rho \equiv mN/V = 1$ and the physical constants are determined by the values of ξ and $c = 2$. Numerical integration of Eq. (3) is performed in a cubic box of length $V^{1/3} = 2\pi$ by using a standard pseudospectral code with an exponential time-splitting temporal scheme (see Table I). Ensemble averaging is done over 30 initial conditions.

To address the KW problem, an array of four alternate-sign vortices is used. To obtain a clean initial condition and reduce initial phonon emission, in a first step, an exact stationary solution of the GPE with straight vortices is numerically obtained by a Newton method [23]. Vortices are separated by a distance π and can be considered isolated when $\xi \rightarrow 0$, as the
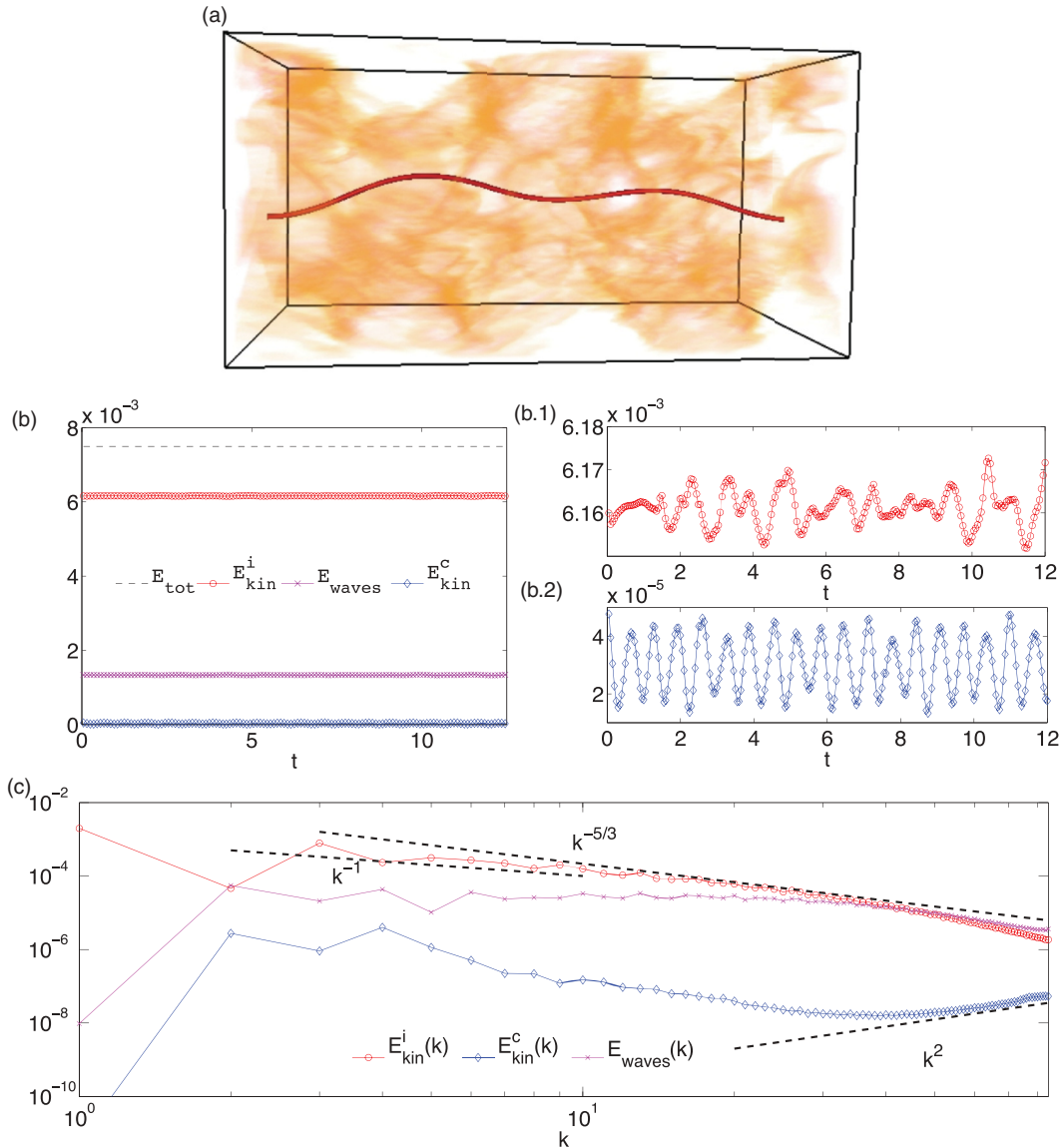

FIG. 1. (Color online) (a) 3D visualization of the density $|\psi|^2$ in the sub-box $[0,\pi]^2 \times [0,2\pi]$. In red an isosurface of the vortex and a (orange) density plot shows sound waves. (b) Temporal evolution of energies. (b.1), (b.2) Zoom of E_{kin}^i and E_{kin}^c, respectively. (c) Incompressible-kinetic, compressible-kinetic, and wave energy spectra. Dashed lines display k^2, k^{-1}, and $k^{-5/3}$ power-law scalings.

resolution is increased. Then, a KW is introduced perturbing the vortex. It reads

$$x(z) = A \sum_{i=1}^{n} \cos\left(i\, z + \phi_i^x\right), \quad y(z) = A \sum_{i=1}^{n} \cos\left(i\, z + \phi_i^y\right),$$

(4)

where $\phi_i^{\{x,y\}}$ are random phases. A visualization of the the density $\rho(\mathbf{x})$ is displayed in Fig. 1(a) at $t = 10$. The KW is observed with the (red) isosurface. Phonon waves correspond to the (orange) cloud that is a density plot of $\rho(x)$ in a narrow threshold centered around the mean-density value $\rho = 1$. In superfluid turbulence, interaction and reconnection between vortices can influence KW propagation. Here such effects are neglected. To quantify the vortical and wave energy of the configuration, we use the standard hydrodynamic energy decomposition, obtained by using the Madelung transformation (see [24] for details). The total energy is thus decomposed in two terms: the incompressible-kinetic energy E_{kin}^i containing the contribution of vortical structures and the energy of phonon waves $E_{\text{wav}} = E_{\text{kin}}^c + E_{\text{int}} + E_q$, where E_q, E_{int}, E_{kin}^c, are the quantum, internal, and compressible-kinetic energy, respectively. Figure 1(b) displays the temporal evolution of E_{kin}^i, E_{kin}^c, E_{wav}, and $E_{\text{tot}} = E_{\text{kin}}^i + E_{\text{wav}}$. Observe in Fig. 1(b) that their temporal evolution rapidly reaches a (quasi)statistical stationary regime. The same energy decomposition can be applied to the energy spectra that are displayed on Fig. 1(c) at $t = 10$. The energy spectrum of the compressible-kinetic energy presents at large wave numbers a k^2-equipartition regime. This range is also present in the initial condition albeit with smaller values. It rapidly reaches the stationary state observed in Fig. 1(c) showing that thermalized waves coexist with vortices. As $E_{\text{wav}} \ll E_{\text{kin}}^i$, the large-scale GPE dynamics is mainly driven by vortices setting a clean configuration.

The energy spectra displayed in Fig. 1(c) present a k^{-1} scaling at small k; this can be associated with decaying of the velocity field of an isolated vortex at long distances [24,25]. At an intermediate range a scaling compatible with $k^{-5/3}$, however, it cannot be associated with Kolmogorov turbulence as the scale separation $V^{1/3} \gg \ell$ is not realized (here $V^{1/3} \sim \ell$). Note that a $k^{-5/3}$ has been also observed in a situation where the Kolmogorov regime is not clear to be applicable [25]. The scaling could be explained by the presence of a KW cascade and predictions (1) or (2), as the principal contribution to energy of the fluid (see Fig. 1) is coming from vortices. However, the relationship between the KW spectrum and 3D (hydrodynamical) energy spectra is not clearly established. To explicitly study the KW cascade, we numerically track the coordinates $(x(z), y(z))$ of the vortex. For each value of z the equation $\psi(x(z), y(z)) = 0$ is solved by using a Newton method. Derivatives of the fields at intermesh points are obtained by Fourier interpolation. This allows us to accurately obtain the vortex coordinates with a precision much larger than the one given by the mesh size. Once the coordinates are obtained, it is possible to compute (1D) KW occupation-number spectrum defined by

$$n(k) = |\hat{w}(k)|^2 + |\hat{w}(-k)|^2,$$

(5)

where $\hat{w}(k)$ is the Fourier transform of $w(z) = x(z) + i\, y(z)$. The KW spectrum allows us to construct the KW energy $E_{\text{KW}} = \sum_k \omega(k) n_k$ and the dissipation $\epsilon = -dE_{\text{KW}}/dt$, where $\omega(k)$ is the KW dispersion relation. It can be approximated by $\omega(k) = C(\kappa/4\pi)k^2$, where C is a numerical constant which eventually depends logarithmically on ξ/ℓ. Figures 2(a) and 2(b) show the temporal evolution of the total vortex length $L = \int \sqrt{1 + |\partial_z w(z)|^2}\, dz$ and the mean curvature $K = \int |\partial_z w(z) \times \partial_{zz} w(z)|/|\partial_z w(z)|^3\, dz$, normalized by their initial values. Note that their temporal fluctuations are small. Finally, in Fig. 2(b) the temporal evolution of the KW
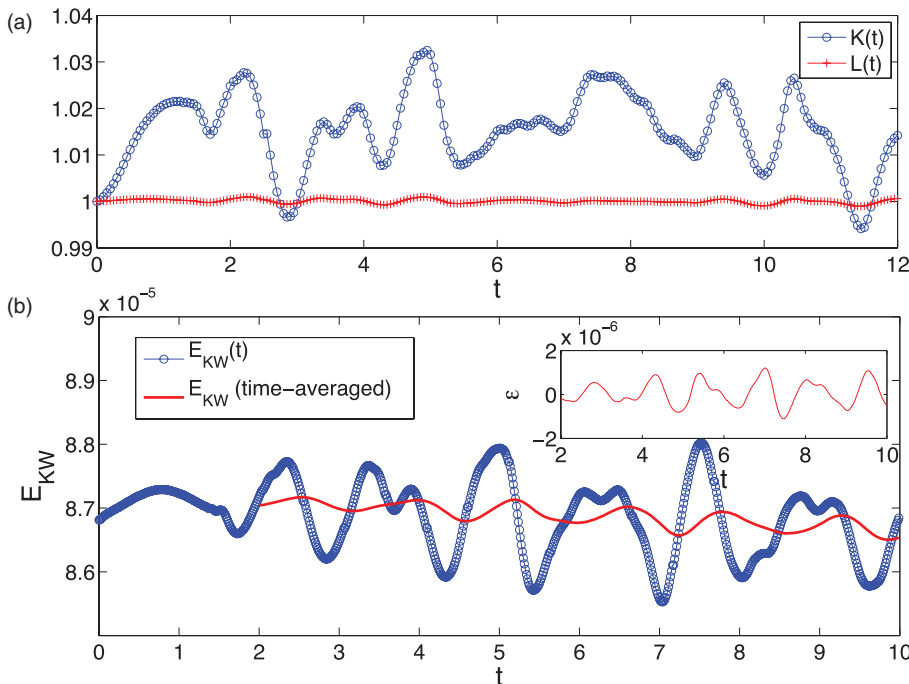

FIG. 2. (Color online) (a) Vortex length $L(t)$ (blue circles) and curvature $K(t)$ (red crosses) normalized by $L(0) = 6.51$ and $K(0) = 0.44$. (b) KW energy $E_{\text{KW}}(t)$ (circles). The (red) solid line displays $E_{\text{KW}}(t)$ averaged over temporal windows of width $\Delta t = 2$. Inset: energy dissipation ϵ.

energy is displayed. Note that the energy fluctuates, especially after the arrival of phonon waves coming from neighboring cells at $t \sim \pi/c \approx 1.5$. The solid (red) line presents the energy averaged over temporal windows of width $\Delta t = 2$; the decrease in energy is apparent. The inset of Fig. 2(b) displays temporal evolution of the energy dissipation showing also some negative values. This can be related to the presence of phonon waves that excite KW at small scales. Its temporal average is positive as more energy is radiated than absorbed by the vortex.

We now turn to the KW spectrum. Two kinds of simulations are presented: the first trying to enhance the scale separation between $V^{1/3}$ and ξ and thus obtaining a larger inertial range; the second concerns the dissipative range of the KW spectrum and then presents a large number of modes between ξ and smallest resolved scale $V^{1/3}/N_z$. Details of runs are listed in Table I.

Let us focus now on the inertial range of the KW cascade. The two KS and LN predictions for $n(k)$ read

$$n_{\mathrm{KS}}(k) = \frac{4\pi C_{\mathrm{KS}} \kappa^{2/5} \epsilon^{1/5}}{k^{17/5}}, \quad n_{\mathrm{LN}}(k) = \frac{4\pi C_{\mathrm{LN}} \epsilon^{1/3}}{\Psi^{2/3} k^{11/3}}, \quad (6)$$

where C_{KS} and C_{LN} are numerical constants. The temporal evolution of the KW spectrum is displayed in Fig. 3(a) for run III. KW are rapidly exited, and populate all wave numbers. At low wave numbers an excess of energy is observed. For Bose gases, a wave-turbulence energy transport to large scales was reported in [26]; here for KW, data do not allow to clearly observe such a behavior. When energy arrives to scales small enough to be efficiently dissipated, a steep decay zone called dissipative range in hydrodynamic turbulence [5] is observed. As dissipation by phonon emission is very weak [27], the spectrum stabilizes and a clear inertial range is observed. For all modes the amplitude of KW remains small; it is thus expected that weak-turbulence theory applies for wave numbers such that $V^{-1/3} \ll k \ll 2\pi/\xi$. Temporal-averaged KW spectrum of runs I–IV are displayed in Fig. 3(b). A power-law scaling is clearly appreciated for almost one decade.

The exponent m, obtained from a fit k^{-m}, is shown on Table I with their respective errors.

For all runs the exponent is slightly larger than the one predicted by the two weak-turbulence results (6) and presents a variation of 5%. However, for all runs data support the exponent $-5/3 - 2$ predicted by LN, that it is within errors, and excludes the $-7/5 - 2$ KS prediction. Note that although the power-law range extends until near $1/\xi$, where dissipation can start to play a role, the exponent m is stable for the different runs. Experimentally, one usually has access only to the (3D) kinetic energy, that for small amplitude KW is dominated by the singularity of the velocity at the vortex core. However, a singularity cannot transfer energy and the KW cascade is thus crucial for understanding low-temperature dissipative mechanisms of superfluids.

We now turn to the dissipative range of the KW spectrum, that takes place at wave numbers larger than $k_\xi = 2\pi/\xi$. For such small scales it is known that dispersive effects of phonon waves slow down the dynamics producing a bottleneck and quasithermalization [28]. This effect was observed for large values of $\xi k_{\max}$, where $k_{\max}$ is the largest wave number. A natural question is can this slowdown affect the dissipative mechanism of the KW cascade? If excitations of high-wave-number phonons are difficult, one could expect that dissipation of KW by sound emission should be reduced at such scales. To investigate such a configuration we have performed simulations with a large value of $\xi k_{\max} = 17$ (run V). For such a configuration, the inertial range of the KW cascade is not clearly identified in Fig. 4(a). At very early times, KWs stop to be populated at wave numbers larger than $k_\xi \sim 60$ displaying an equipartition of KW spectrum followed by a faster than exponential decay for $k > k_\xi$. Unlike, the 3D dispersive bottleneck, this behavior does not last long and the statistics of KW modes in this range is not Gaussian. At later times, the equipartition range is destroyed and a large-k exponential decay of rate $2 \delta(t)$ [see Fig. 4(a)] is observed.

Finally we study the statistics of KW amplitudes in the inertial and dissipative range. The PDF of KW amplitudes
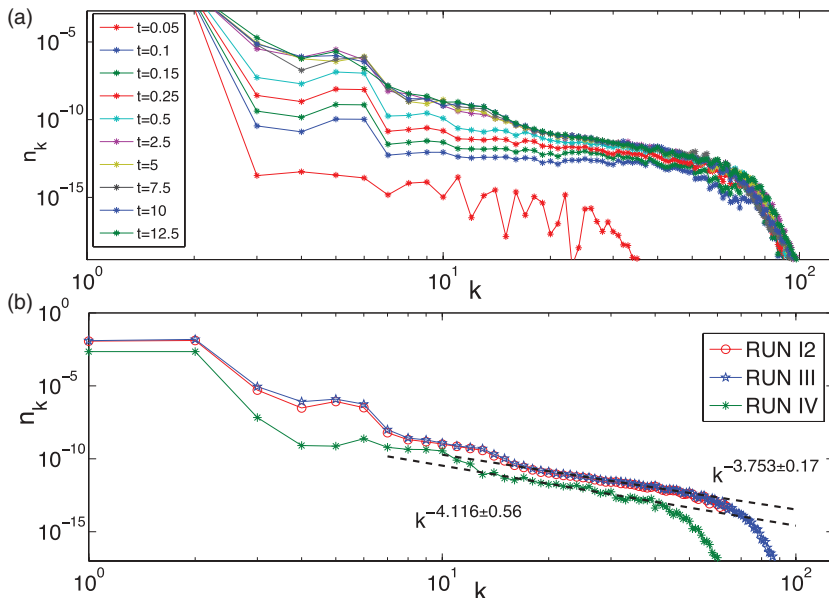

FIG. 3. (Color online) (a) Temporal evolution of KW spectrum, run III. (b) Time-averaged KW spectra, runs I–V. Dashed line displays the power-law fits.
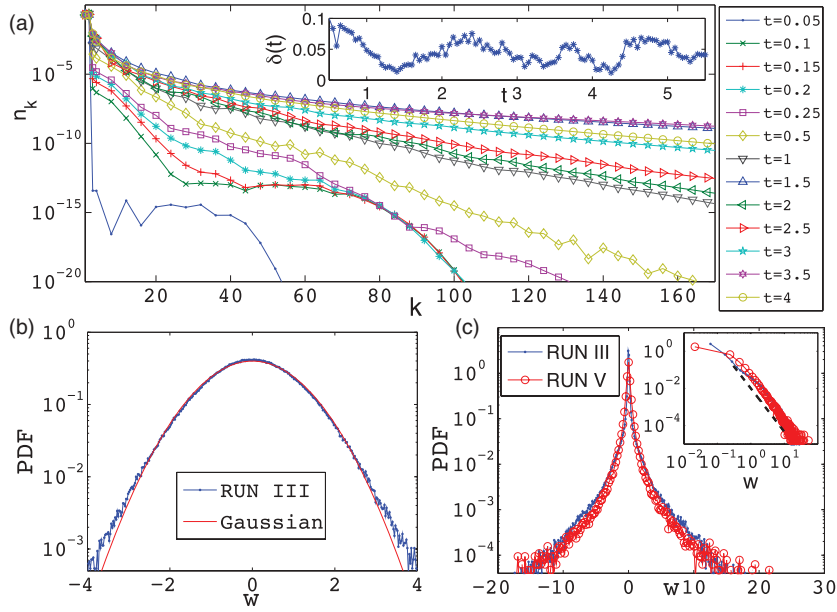
FIG. 4. (Color online) (a) Temporal evolution of KW spectrum for run V. Inset: temporal evolution of the exponential decay rate $\delta(t)$. (b) PDF of KW amplitudes in the inertial range $20 < k < 40$ (run III). (c) PDF of KW amplitudes in the dissipative range $80 < k < 100$ (run III) and $30 < k < 170$ (run V). Inset: same PDF in log-log, the power law $w^{-7/3}$ is drawn for reference.

varying at scales inside the inertial range for run III is obtained by filtering in Fourier space and keeping modes in the range $20 < k < 40$. The normalized PDF is displayed in Fig. 4(b). The quasi-Gaussian behavior is manifest as expected from weak turbulence predictions. $|w(z)|^2$ consequently presents exponential tails. In the dissipative range (for $80 < k < 100$) the PDF shows a strong non-Gaussian character as apparent in Fig. 4(c). Better statistics are obtained for run V. The PDF has power-law tails as shown in the inset of Fig. 4(b) and present, as in turbulent flows, an asymmetry of skewness $\langle w^3 \rangle / \langle w^2 \rangle^{2/3} = -0.15$. Recently, in Biot-Savart simulations [29], a crossover between Gaussian and non-Gaussian statistics was found in the velocity field at the mean intervortex scale ℓ. Here, for KWs, the crossover takes place at the scale $\xi \ll \ell$. At scales smaller than ξ, KWs are somehow decoupled of the large-scale dynamics prescribed by wave turbulence and are in direct interaction with a strongly fluctuating superfluid velocity field, as the one found in the GP simulations of Ref. [30], and hence inherit some properties of the surrounding fluid.

The behavior of KWs at very small scales is important at low temperature where mutual friction is absent. In all vortex-filament models, some small-scale artificial dissipation is needed to avoid energy pileup. Although vortex-filament models are not concerned with such small scales, how the energy is dissipated in those models can affect the vortex dynamics. It would be important to check if the dissipative mechanisms used are consistent with dissipation produced by phonon radiation. A natural extension of this work is to include thermal waves and vortex interaction by using the projected GPE, where mutual friction effects are present [31].

[1] E. A. L. Henn J. A. Seman, G. Roati, K. M. F. Magalhaes, and V. S. Bagnato, Phys. Rev. Lett. **103**, 045301 (2009).

[2] D. I. Bradley, S. N. Fisher, A. M. Guénault, R. P. Haley, G. R. Pickett, D. Potts, and V. Tsepelin, Nat. Phys. **7**, 473 (2011).

[3] V. Eltsov *et al.*, Phys. Rev. Lett. **99**, 265301 (2007).

[4] G. P. Bewley, D. P. Lathrop, and K. R. Sreenivasan, Nature (London) **441**, 588 (2006).

[5] U. Frisch, *Turbulence: The Legacy of A. N. Kolmogorov* (Cambridge University Press, Cambridge, 1995).

[6] J. Maurer and P. Tabeling, Europhys. Lett. **43**, 1 (1998).

[7] C. Nore, M. Abid, and M. E. Brachet, Phys. Rev. Lett. **78**, 3896 (1997).

[8] J. Yepez, G. Vahala, L. Vahala, and M. Soe, Phys. Rev. Lett. **103**, 084501 (2009).

[9] W. F. Vinen and J. J. Niemela, J. Low Temp. Phys. **128**, 167 (2002).

[10] W. Thompson (Lord Kelvin), Philos. Mag. **10**, 155 (1880).

[11] V. Zakharov, V. Lvov, and G. Falkovich, *Kolmogorov Spectra of Turbulence I—Wave Turbulence* (Springer-Verlag, Berlin, 1992).

[12] J. Laurie, V. S. Lvov, S. Nazarenko, and O. Rudenko, Phys. Rev. B **81**, 104526 (2010).

[13] V. V. Lebedev and V. S. L'vov, J. Low Temp. Phys. **161**, 548 (2010).

[14] E. V. Kozik and B. V. Svistunov, J. Low Temp. Phys. **161**, 603 (2010).

[15] V. V. Lebedev, V. S. L'vov, and S.V. Nazarenko, J. Low Temp. Phys. **161**, 606 (2010).

[16] E. B. Sonin, Phys. Rev. B **85**, 104516 (2012).

[17] L. Boué, R. Dasgupta, J. Laurie, V. L'vov, S. Nazarenko, and I. Procaccia, Phys. Rev. B **84**, 064516 (2011).

[18] E. V. Kozik and B. V. Svistunov, Phys. Rev. Lett. **92**, 035301 (2004).

[19] V. S. L'vov and S.V. Nazarenko, J. Low Temp. Phys. **36**, 785 (2010).

[20] E. V. Kozik and B. V. Svistunov, Phys. Rev. Lett. **94**, 025301 (2005).

[21] A. W. Baggaley and C. F. Barenghi, Phys. Rev. B **83**, 134509 (2011).

[22] W. F. Vinen, M. Tsubota, and A. Mitani, Phys. Rev. Lett. **91**, 135301 (2003).

[23] C. Huepe and M. Brachet, Physica D **140**, 126 (2000).

[24] C. Nore, M. Abid, and M. Brachet, Phys. Fluids **9**, 2644 (1997).

[25] B. Nowak, J. Schole, D. Sexty, and T. Gasenzer, Phys. Rev. A **85**, 043627 (2012).

[26] J. Schole, B. Nowak, and T. Gasenzer, Phys. Rev. A **86**, 013624 (2012).

[27] G. Krstulovic, M. Brachet, and E. Tirapegui, Phys. Rev. E **78**, 026601 (2008).

[28] G. Krstulovic and M. Brachet, Phys. Rev. Lett. **106**, 115303 (2011).

[29] A. W. Baggaley and C. F. Barenghi, Phys. Rev. E **84**, 067301 (2011).

[30] A. C. White, C. F. Barenghi, N. P. Proukakis, A. J. Youd, and D. H. Wacks, Phys. Rev. Lett. **104**, 075301 (2010).

[31] G. Krstulovic and M. Brachet, Phys. Rev. E **83**, 066311 (2011).